Modeling elastic properties in carbonate rocks

Shiyu Xu and Michael A. Payne, ExxonMobil

Carbonate (limestone and dolomite) reservoirs account for approximately 50% of oil and gas production worldwide. However, seismic responses in carbonate rocks are poorly understood. In addition, DHI ranking and AVO classification systems developed for clastic rocks are unlikely to be applicable to carbonate rocks. An accurate and physically sound carbonate rock physics model is needed to address these technical issues.

Development of a carbonate rock physics model is extremely difficult because pore systems are more complex in carbonate rocks than they are in clastics. While clastic rocks have mainly intergranular pores, carbonate rocks can have a variety of pore types, such as moldic, vuggy, interparticle, and intraparticle. Diagenesis often plays a significant role in the development of such a pore system. The complex pore system makes the porosity-velocity relationship highly scattered. Recent experimental results indicate that pore type can cause as much as a 40% change in P-wave velocity for a given porosity. Pore shape appears to be the dominant factor in carbonate rock physics. In general, moldic, intraframe, and vuggy pores tend to be rounded and make the rock stronger (faster) than when the pores are interparticle. On the other hand, micropores, e.g., microcracks, tend to be flat and make the rock weaker. To effectively characterize carbonate reservoir rocks, it is critical to develop a rock physics model capable of handling different pore types.

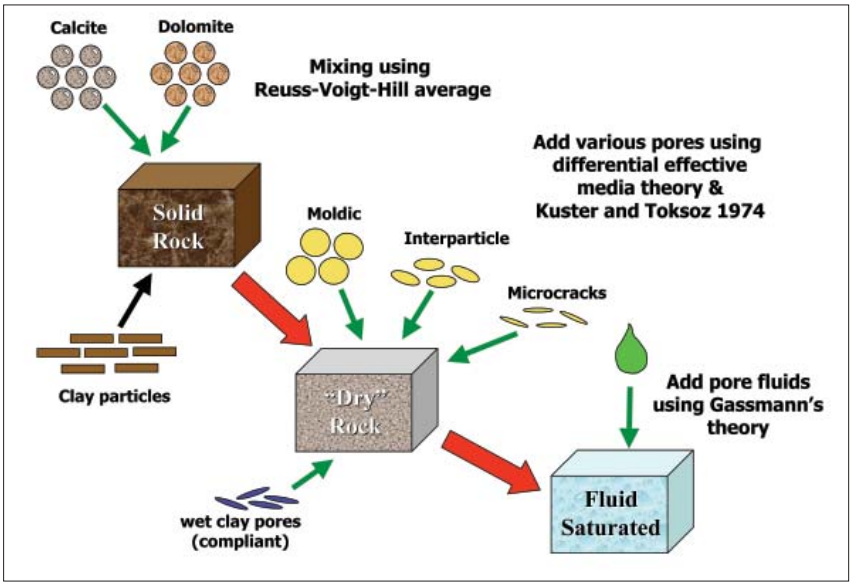

Figure 1. *Diagram of our carbonate rock physics model.*

Gassmann fluid substitution is a powerful tool for AVO analysis and 4D interpretation, but Gassmann's theory requires many assumptions. Among them, a fundamental assumption is that pore pressure will be equilibrated (or quasi-equilibrated) within a half cycle of the seismic wave. In practical applications, this assumption can be violated due to many factors such as permeability (global and/or local), fluid viscosity and compressibility, pore structure, compressibility of pore space, heterogeneity, and wettability of the rock. The complex, multiscale pore system in carbonates leads some authors to question the applicability of traditional Gassmann fluid substitution while others claim that the Gassmann theory works perfectly fine. It is important to understand why Gassmann may work in some cases but not in others.

Due to the brittle nature of carbonate rocks, fractures are more prevalent than in clastics. These fracture systems act as conduits for fluid flow and can considerably enhance hydrocarbon production in low-porosity carbonate rocks or tight gas sands. However, modeling the effect of fractures on the seismic response can be very tricky. For example, some fracture models often ignore mechanical interactions between fractures. This type of fracture model can provide inaccurate results, even though it may successfully explain the observed elastic behavior. Most fracture models also assume isolated pores and, hence, are unable to account for the effect of pore fluid pressure relaxation on the seismic response. It is dangerous to apply this type of fracture model to interpret, say, low-frequency seismic data. Finally, almost all proposed fracture models do not handle other types of anisotropy, such as shale anisotropy and layering anisotropy. In practice, different types of anisotropy often co-exist; e.g., fractured geobodies (carbonates or sandstone) are often interbedded with shales. There is a business need to develop a fracture model that is able to handle various types of anisotropy consistently.

A very good discussion on various rock physics modeling issues was given by Sayers (2008). In this article, we share our experience in this area. First, we extend the Xu-White model, originally designed for clastic rocks, to carbonates by accounting for a variety of pore types. Second, we propose a procedure for estimating pore types from velocity and porosity data, following the work of Kumar and Han (2005). The pore-type effect on Gassmann fluid substitution is then discussed. Finally, we incorporate anisotropy, both due to fractures and to shale, in our model. In particular, we focus on the effect on elastic properties including anisotropy of fluid communication among matrix pores and fractures.

Carbonate rock physics model

Empirical rock physics models are widely used in the industry, due to their simplicity. These models typically assume a linear relationship between P-wave (or S-wave) velocity and porosity. Despite some limited success of such models, we question their applicability to seismic inversion, since they are highly data-driven. Another major drawback to empiri-

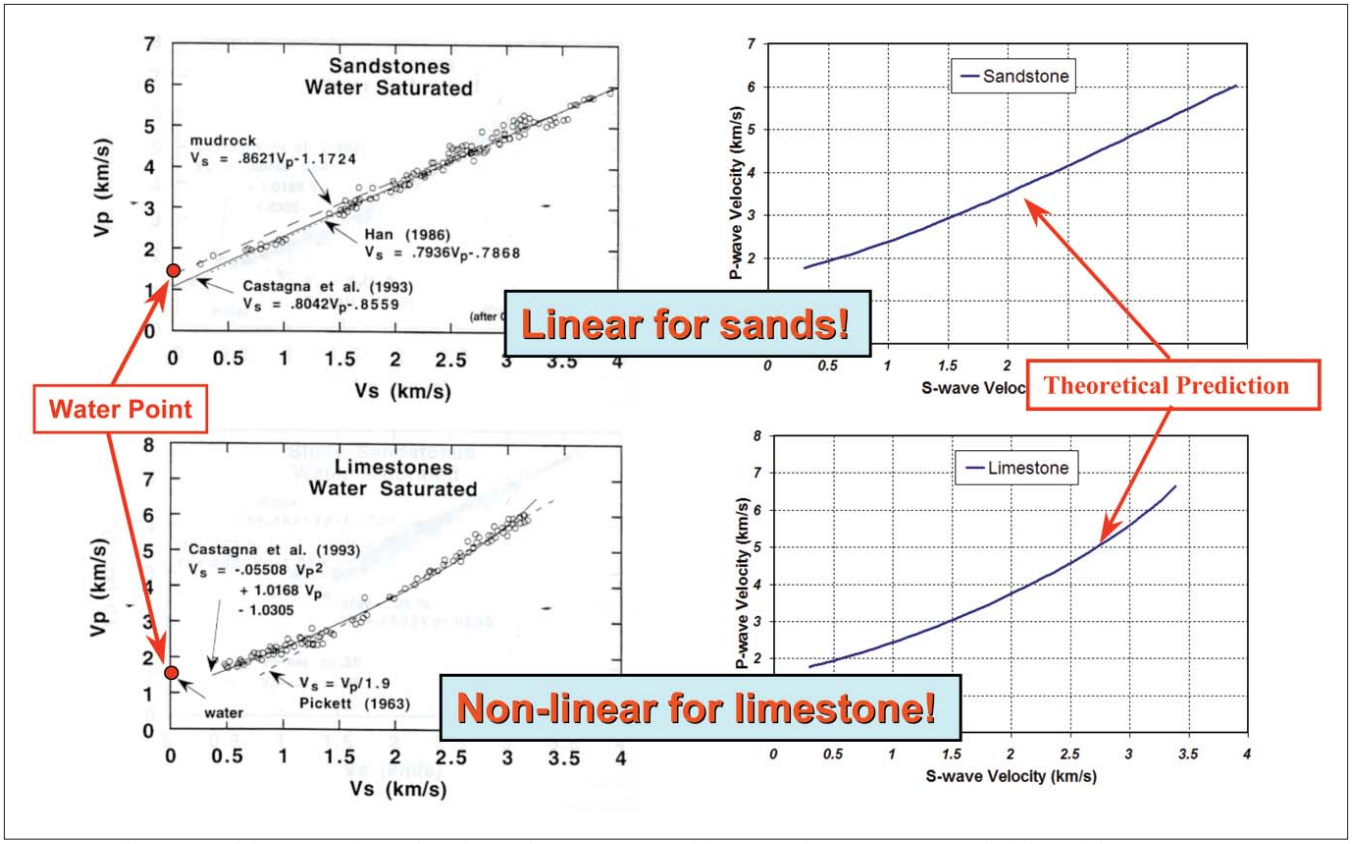

Figure 2. *Illustration of the V_p-V_s relationships for sandstone (upper) and limestone (lower). Figures on the left are laboratory measurements and those on the right are our predictions. (Left figures from Castagna et al.)*

cal models is that they provide us with little physical insight. Finally, an empirical model can handle only a very limited number of factors (typically fewer than three).

In this paper, we extend the Xu-White model to carbonate rocks. In the model, the total pore volume is divided into four pore types: (1) clay-related pores, (2) interparticle pores, (3) microcracks, and (4) stiff pores:

$$\phi_T = \phi_{Clay} + \phi_{IP} + \phi_{Crack} + \phi_{Stiff} \quad (1)$$

We partition the pore space into clay and nonclay pores using the method proposed by Xu and White (1995):

$$\phi_{Clay} = V_{sh}\phi_T \quad (2)$$

where Vsh is the shale volume, which is normalized by the total volume of grain matrix. Despite the fact that carbonate rocks are generally clean, we keep clay pores in the model to make it applicable in a mixed carbonate-clastic environment.

Microcracks represent the most compliant component in rocks, whether in clastics or carbonates. As a result, they are extremely sensitive to stress. We use the following equation to relate crack porosity ϕ_{crack} to effective stress σ_e:

$$\phi_{Crack} = \phi_{Init} e^{-\beta\sigma_e} \quad (3)$$

where ϕ_{Init} denotes initial crack porosity at zero effective overburden stress σ_0, and β is a constant. ϕ_{Init} and β can be estimated from stress-dependent P- and S-wave velocities measured in the laboratory. In the case of deviatoric stress, microcracks may be aligned by the differential stress (defined as the difference between the maximum and minimum principal stresses). The preferred orientation distribution will govern the anisotropic behavior of the rock.

The stiff pores (ϕ_{stiff}) generally represent the rounded moldic pores or vugs in carbonate rocks. Finally, the interparticle pores (ϕ_{IP}) make up the dominant pore space in sedimentary rocks. They are, in general, insensitive to stress and have no preferred orientation.

Figure 1 shows how the model works. Our method consists of four steps.

1) The minerals present in the rock are mixed using a mixing law (e.g., the Reuss-Voigt-Hill average). We begin with a solid rock matrix having the properties of this mixture.

2a) Micropores with bound water (e.g., clay pores) are added to the matrix using the differential effective medium or DEM (Xu and White, 1996) process and the Kuster-Toksöz theory (1974) to account for the mechanical interaction between the pores. The calculated effective elastic properties (e.g., bulk modulus) will be used later as the "solid" properties for fluid substitution.

2b) Go back to step 2a. All pores including water-wet micropores and empty (or dry) nonbound-water pores are added into the system using the effective medium theory to provide the effective elastic properties (e.g., bulk modu-

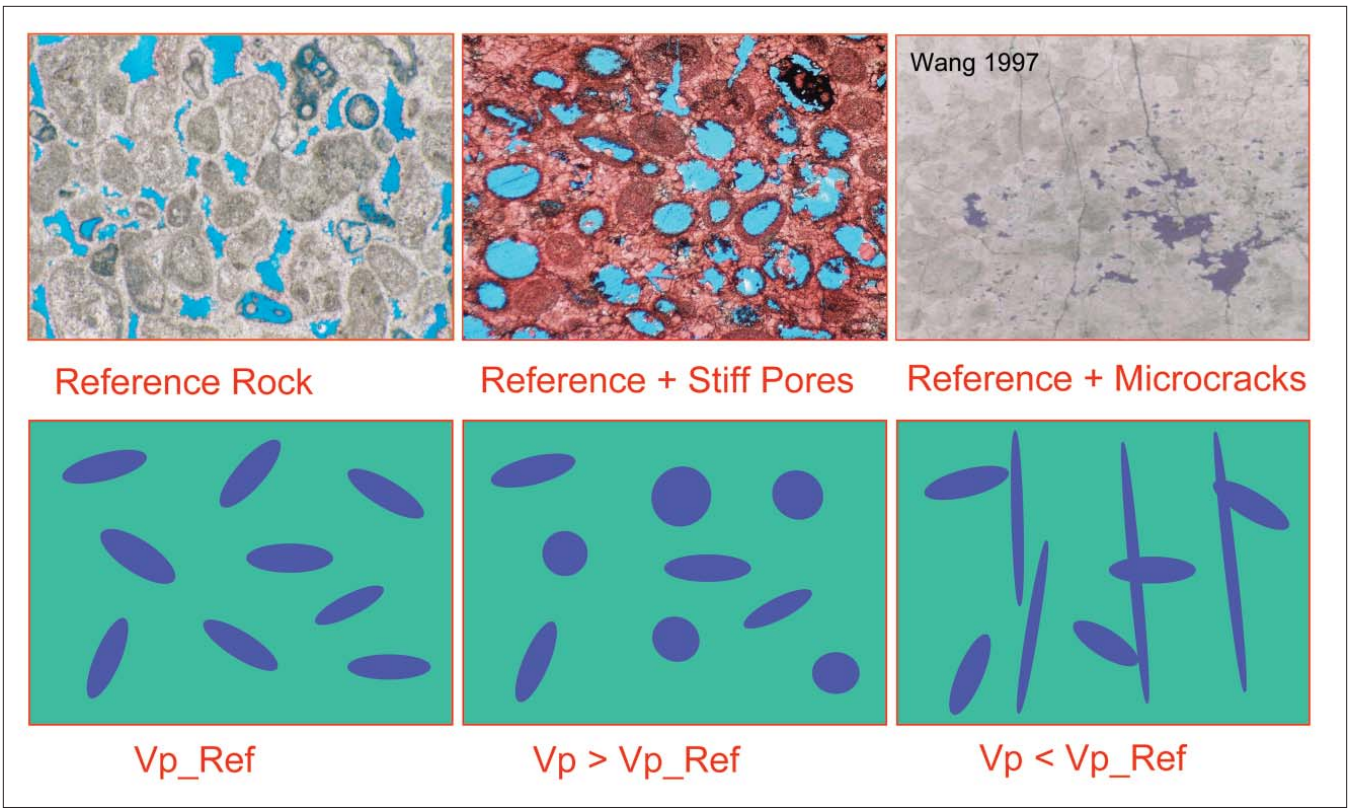

Figure 3. *Illustration of different pore types in carbonate rocks and how to model them. The third thin section was taken from Wang (1997).*

lus) of the "dry" rock frame.

3) The remaining water (which is not bound to micropores) is mixed with the hydrocarbons (oil or/and gas) using a fluid mixing law such as the Wood suspension model.

4) Gassmann's equations are used to add the fluid mixture into the pore system in order to obtain the final effective elastic properties for the saturated rock.

This approach assumes that macropores (e.g., interparticle) are well-connected and their effective permeability is high enough that pore-pressure differences between these pores will be equilibrated within a half cycle of a seismic wave. On the other hand, water-wet micropores will behave as if isolated from each other due to their extremely small sizes, resulting in a high-frequency seismic response.

Shear-wave log prediction

We follow the procedures described by Xu and White (1996) to predict shear-wave logs from P-wave and shale volume logs. To do this, we first invert porosity from P-wave and shale volume logs using our rock physics model. Then we calculate P-wave, S-wave, and density logs using the inverted porosity. It is important to keep the parameters unchanged during the backward and forward calculation processes. The calculated P-wave log should be exactly the same as the measured log, but the S-wave and density logs are totally calculated. If a reliable porosity curve is available, we may want to invert rounded pores and microcracks using the method described in the next section and then predict the S-wave log.

To correctly predict the S-wave log, it is crucial to have the right V_P-V_S relationship. Castagna et al. (1993) observed a linear V_P-V_S relationship for sandstone and a highly nonlinear relationship for limestone (left of Figure 2). They then proposed a three-term, nonlinear empirical relation for S-wave velocity prediction in limestone and a two-term, linear relationship for sandstone. The right side of Figure 2 shows our predictions based on our rock physics model. In this case, we assumed a single pore type (no stiff pores or microcracks). All parameters remained the same in the two cases except the mineralogy. We assumed the solid grain to be quartz in the sandstone case and calcite in the limestone case. Our rock physics model predicts a rough linear relationship for sandstone and a highly nonlinear relationship for limestone, without introducing any extra parameters. In fact, a careful look at the sandstone data indicates a slightly nonlinear relation for sandstone, especially for the high-porosity (low-velocity) samples. Also note that the empirical linear trends are unable to predict the 100% water point. The successful prediction of this behavior strongly indicates the power of a theoretical rock physics model. Using a similar approach, Sayers (2008) modeled the effect of pore aspect ratio on the V_P-V_S relationship.

Pore-type effect and its quantification

As discussed earlier, our clean carbonate rock physics model includes three pore types: (1) interparticle pores, (2) the rounded stiff pores that represent moldic pores, intraframe, or vugs, and (3) microcracks that represent the most compli-

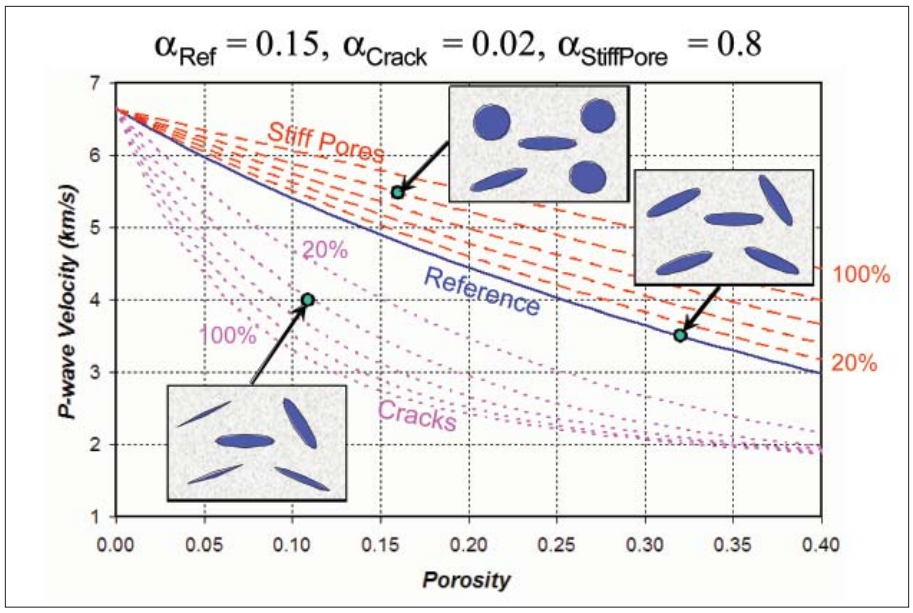

Figure 4. *Predicted effect of pore type on P-wave velocity. We assume that the solid matrix is calcite. α is the aspect ratio. The reference curve represents a system with only interparticle pores. The curves below the reference represent systems with increasing fractions of crack-type pores and those above it represent increasing fractions of stiff pores.*

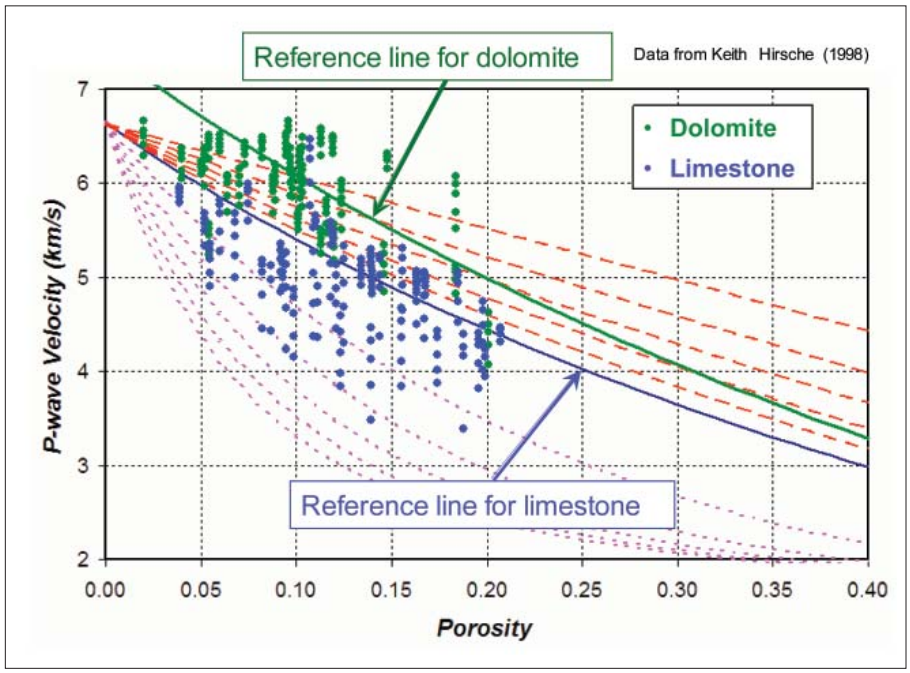

Figure 5. *Illustration of possible pore-type effect on P-wave velocity using laboratory data by Wang et al. (1991). As in Figure 7, the dashed curves above the limestone reference curve indicate increased fractions of stiff pores, and those below indicate increased fractions of cracks.*

ant pores in the system, such as fractures. Each pore type is characterized by a specific pore aspect ratio (the short axis to the long axis ratio). If needed, our model can be easily extended to handle more than three pore types. In practice, however, the three-pore-type model is usually sufficient.

Following Kumar and Han (2005), we assume that the interparticle pore is the most common pore type in carbonate rocks and, therefore, gives a reference porosity-velocity trend. For samples with P- or S-wave velocity above the trend, we suspect a mix of interparticle and rounded (stiff) pores. On the other hand, we suspect a mix system of microcracks and interparticle pores if a data point is below the reference line. Figure 3 shows the concept.

Figure 4 shows the calculated P-wave velocity as a function of porosity and pore type. As expected, for a given porosity, rounded pores make the velocity faster, and microcracks make it slower. With the help of the model, we are able to invert rounded pores or microcracks from P-wave velocity and porosity measurements. For example, a data point lying on the reference line means that there are no rounded pores or microcracks in the system and all pores are interparticle. A data point on the 80% rounded pore line means that 80% of the total pore space is rounded and the remainder is interparticle.

We tested the concept of inferring pore type using laboratory data (Wang et al., 1991). Theoretically, the 100% rounded pore line should give an upper bound, the 100% crack line should give a lower bound, and all data points should fall between the two bounds (Figure 5). In reality, we found some data points sitting well above the upper bound. This can be explained by mineralogy differences. Based on the grain density data, we are able to separate dolomite samples (green) from limestone samples (blue). Because P-wave velocity in dolomite is faster than that in limestone, the reference line for dolomite is well above the reference line for limestone. Excluding data points from dolomite samples, all data points, except three from one limestone sample, are within the bounds. This indicates the importance of correctly handling the mineralogy effect before pore-type inversion. The mineralogy correction can be easily done using our rock physics model. In the case of mixed mineralogy, we mix different solid grains using a mixing law (such as Hill average) to account for the mineralogy effect.

The University of Miami CSL database (Anselmetti and Eberli, 1993, 2001; Baechle et al., 2004; Eberli et al., 2003) was used to test our pore-type inversion method. We noticed some data points sitting below the lower bound. This could be due to either a mineralogy effect or simply errors in the

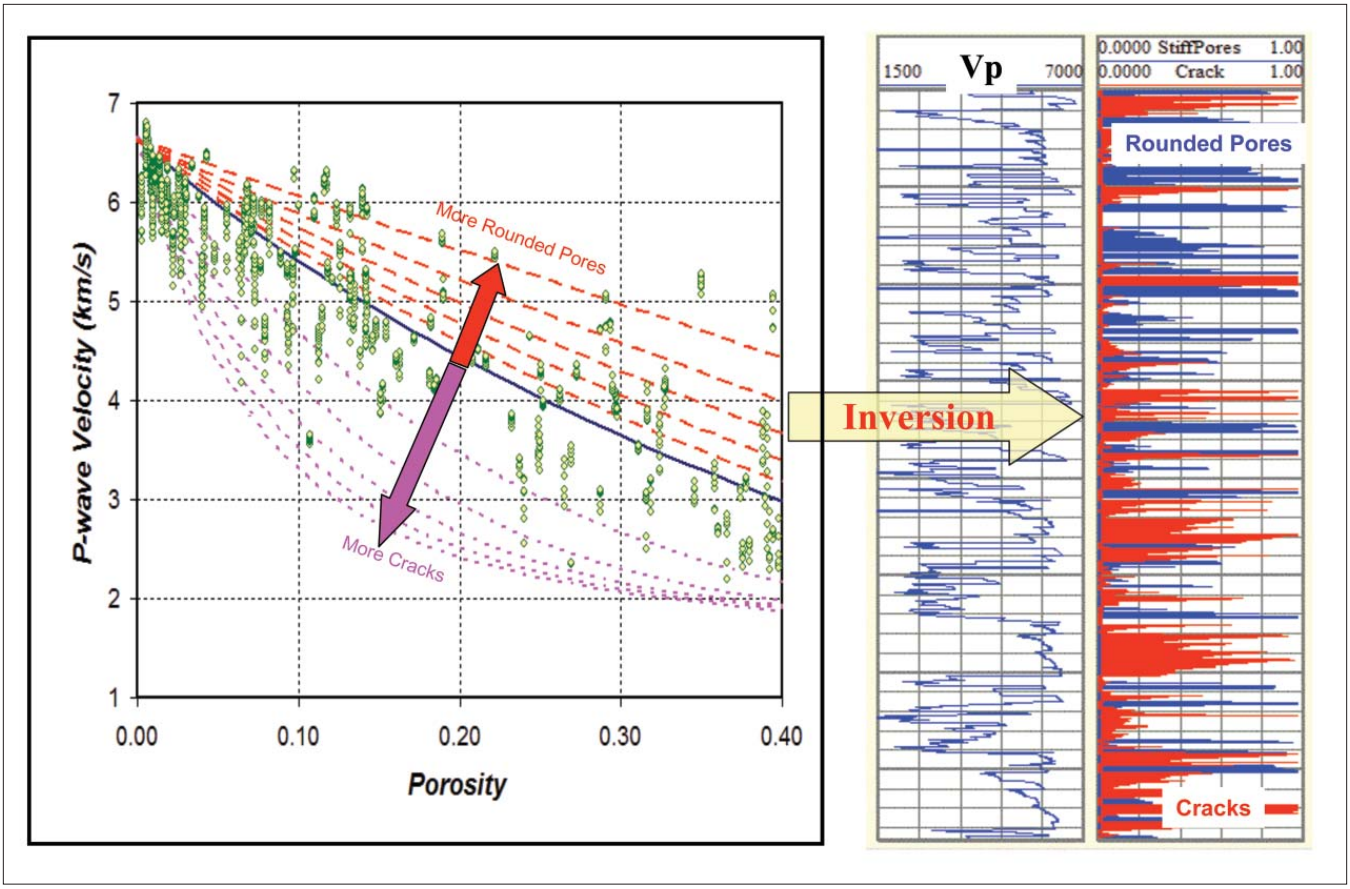

Figure 6. *Illustration of the inverted rounded (stiff) pores and microcracks from the University of Miami data.*

measurements. The inverted rounded pores (blue) and microcracks (red) are shown in Figure 6. It is interesting to see the huge variation in pore type from sample to sample. In some cases, rounded pores dominate the pore space, and in others, crack-like compliant pores dominate. When working with field data, it would be important to see how the inverted pore types linked to geology.

Above, we demonstrated how to quantify the pore-type effect using P-wave velocity data. Using the theoretical framework presented in this paper, we easily extended the method to S-wave velocity data and, furthermore, developed a joint inversion method to invert pore types from the combined P- and S-wave velocity data.

Fluid substitution in carbonate rocks

Here, we show an example to demonstrate a possible pore-type effect on Gassmann fluid substitution. Using the pore-type inversion method described earlier, we can quantitatively estimate how much of the total pore space consists of microcracks. Based on our inversion results using laboratory data, we demonstrate how microcracks might affect Gassmann fluid substitution. The left of Figure 7 is a crossplot of values of measured P-wave velocity in the water-wet samples and that calculated from dry rock properties using Gassmann's equations. If Gassmann's theory worked perfectly, all data points would lie on the diagonal line (red). In reality, most of the data points lie below the diagonal line, indicating the Gassmann-predicted P-wave velocity is slower than the measured velocity. To demonstrate the microcrack effect, we color-coded the data points using the inverted crack porosity. We note that Gassmann tends to underpredict P-wave velocity in samples with more microcracks. This is understandable since microcracks have very low local permeability because of their extremely small sizes. Pore fluid (water) tends to be trapped in these microcracks and pore pressure is unable to relax within a half cycle of the wave. This causes a violation of the fundamental Gassmann assumption.

As we mentioned earlier, our rock physics model is able to add water into the system within the micropores using the inclusion-based theory without applying Gassmann fluid substitution to those pores. We call this non-Gassmann fluid substitution. We reperformed the fluid substitution by assuming isolated microcracks, but with the other pores perfectly connected. In this case we have a mixed system consisting of Gassmann-consistent macropores and non-Gassmann-consistent microcracks with unrelaxed pore fluid. After the treatment, we observed that the high-crack porosity data points moved much closer to the perfect prediction line (right of Figure 7).

This is a very important finding since it demonstrates that Gassmann's assumption of equalized pore pressure tends to be violated more easily in rock samples with multipore types. This is because (1) local-scale pore-pressure gradients exist only if stiff pores and compliant pores coexist, and (2) the

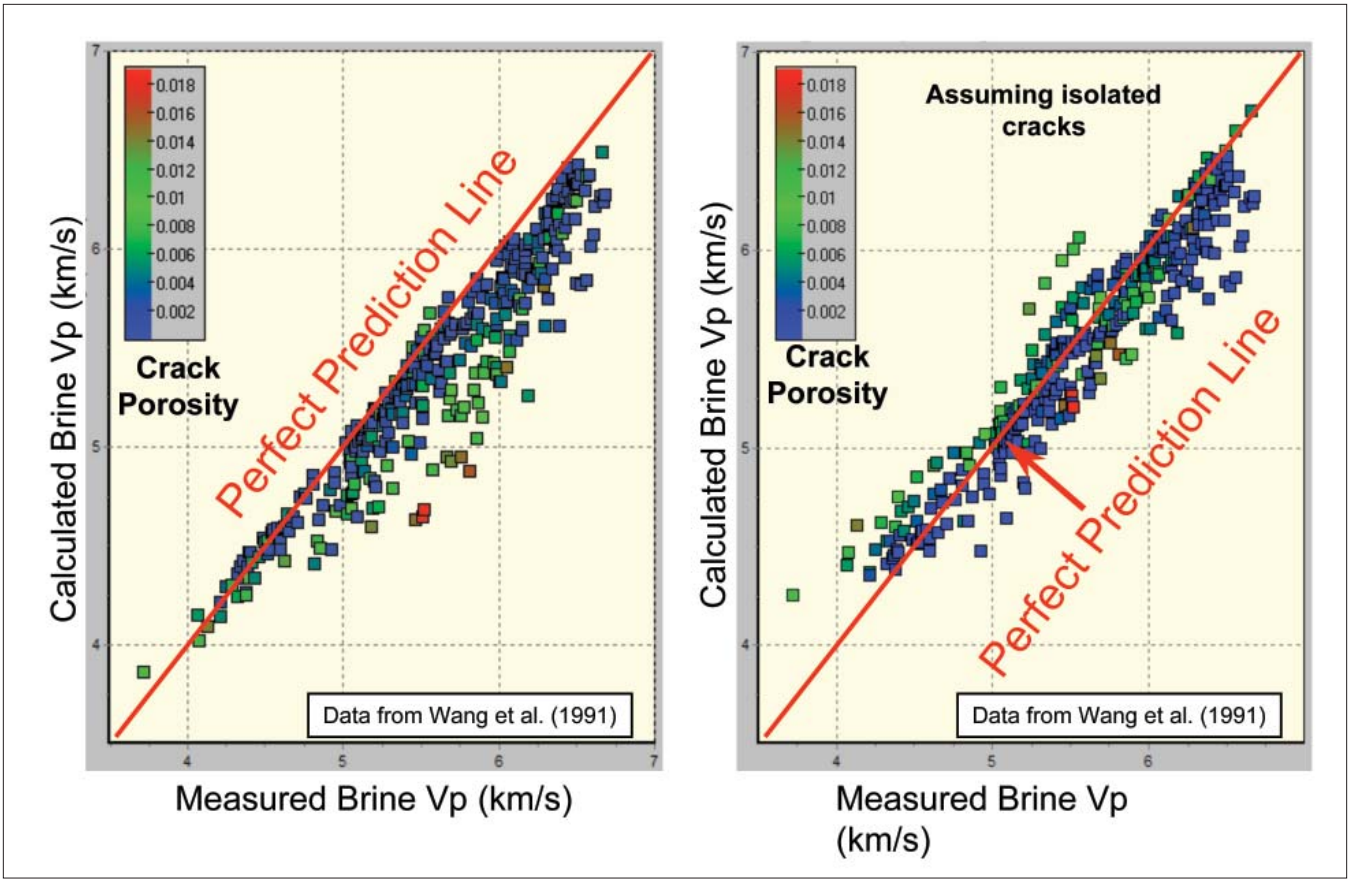

Figure 7. *(left) Illustration of effect of microcracks on Gassmann fluid substitution in carbonate rocks. (right) Crossplot using both Gassmann (for macropores) and non-Gassmann (for cracks) fluid substitution. The data points are color-coded using microcrack porosity estimates from our pore-type inversion method.*

local permeability is low due to the extremely small size of micropores, which tends to restrict or slow down pore-fluid pressure relaxation.

Modeling fracture effect

The workflow for anisotropic rock physics modeling is almost the same as that for the isotropic case (Figure 1), except that an anisotropic effective medium theory (e.g., the anisotropic dry-rock approximation proposed by Xu et al., 2006), rather than the Kuster-Toksöz theory, will be used to add pores into the system. Also note that we use the anisotropic Gassmann equations to do the fluid substitution at step 4. In particular, our rock physics model handles anisotropy up to orthorhombic symmetry. It can, therefore, simulate both fracture anisotropy and shale anisotropy consistently. It is not feasible to give all the details about the fracture model and its workflow in this short article, but its main features are summarized below:

1) The model is accurate since it considers the mechanical interactions among fractures and matrix pores.
2) The use of the anisotropic dry rock approximation (Xu et al.) dramatically improves the computational efficiency.
3) The model is able to handle the fluid interactions among fractures and matrix pores and is, therefore, consistent with Gassmann theory at low frequencies.
4) The model can simulate both fracture anisotropy and shale anisotropy.
5) The model can handle up to two sets of fractures.
6) In each fracture set, fractures need not be perfectly aligned. The fracture orientation can be described using, say, a normal distribution.

Due to the lack of well-controlled laboratory experiments on fracture samples, it is difficult to validate any fracture model. However, examples are given below to demonstrate how the fracture model works in practice.

Well logs from an East Texas carbonate gas field were used to test the model (Figure 8). The blue curve in track 1 is the shale volume calculated from the gamma ray log. In general, shale volume calculated from the gamma-ray log is not reliable in carbonate rocks because of the presence of organic matter. This is not a big concern to us in this particular case since we just want to demonstrate how our rock physics model works. The magenta curve in track 2 is the proposed fracture-porosity log. We assumed no fracture (zero fracture porosity) above 3950 ft, but a single fracture set with a symmetry axis parallel to the X axis below that depth. Full elastic tensors were calculated using our fracture model. However, only C11 (blue in tracks 3 and 4), C22 (red in tracks 3 and 5), and C33 (green in tracks 4 and 5) are plotted to show the anisotropic behavior of the rocks. Over the shallow depth interval (above

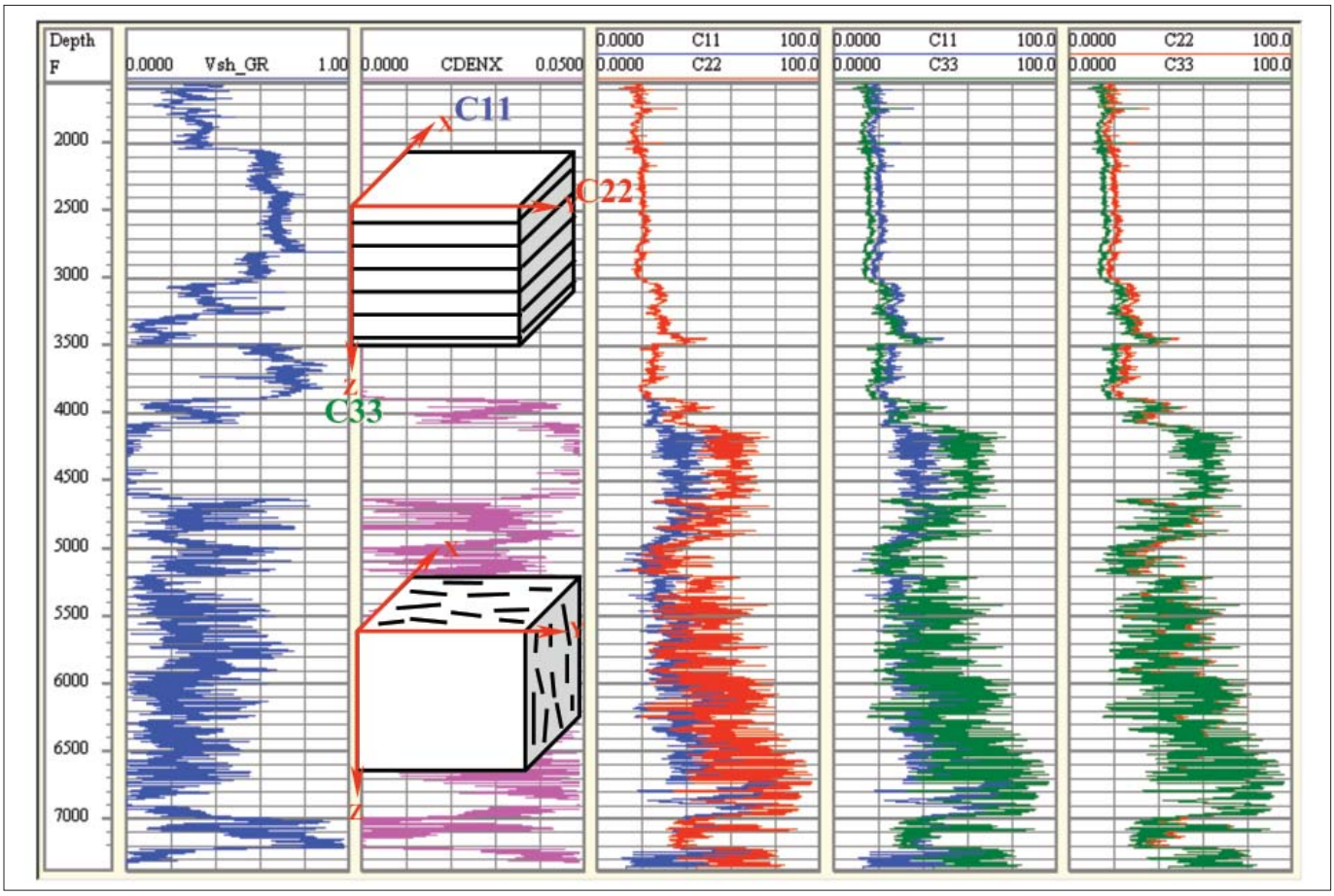

Figure 8. *Illustration of the effect of a single vertical fracture set on seismic anisotropy. Vsh_GR is shale volume estimated from the gamma-ray log, CDENX is fracture density in x direction, C11 (blue), C22 (red), and C33 (green) are elastic constants in x, y, and z directions, respectively.*

3950 ft), fracture density is zero. All the calculated anisotropy comes from shale anisotropy, which is VTI in this case. C11 is the same as C22 but different from C33. Below 3950 ft, the fracture density varies with shale volume. In the clean limestone layers, the fracture anisotropy dominates the elastic behavior and the resulting anisotropy is transversely isotropic with a horizontal symmetry axis (HTI). In this case, C11 is different from C22, but C22 is the same as C33. In the dirty limestone layers, the resulting anisotropy is a combination of shale and fracture anisotropy, giving an orthorhombic symmetry. In this case, all three elastic constants (C11, C22, and C33) are different.

Figure 9 is the same as Figure 8, except that we have two fracture sets, rather than one, below 3950 ft. The second fracture set has fracture densities half that of the first fracture set. The elastic behavior above 3950 ft is still the same, but the azimuthal anisotropy below 3950 ft is much weaker than with one set of fractures. We now see that C22 is very different from C33 but the difference between C11 and C33 is smaller. Our modeling results show that azimuthal seismic anisotropy can be best used to detect fractures if we have one single set of fracture. Azimuthal anisotropy can be very weak if we have two or more sets of fractures.

Conclusions

We extended the Xu-White model, originally designed for clastic rocks, to carbonate rocks. Our new model includes two more pore types (shapes): rounded pores and microcracks. Our model correctly predicts the V_P-V_S relationships for both clastics and carbonates. We also developed a pore-type inversion method based on the model and were moderately successful in inferring pore types in the University of Miami laboratory data set. This study also indicated the complexity of pore types in carbonate rocks.

With the help of our pore-type inversion method, we are able to quantify the effect of microcracks on Gassmann fluid substitution. Our results show that pore fluid in microcracks tends to be unrelaxed, at least at ultrasonic frequencies, probably due to the low local permeability for these cracks. A mixed-mode fluid substitution, assuming the microcracks are isolated while the rest of the pores are perfectly connected, gives a much better match between calculated and measured P-wave velocities.

Using the predicted S-wave logs, we are able to quantify the effect of mud filtrate invasion on sonic logs. Although not shown here, application of the method to many wells in carbonate fields worldwide resulted in significant improvement in seismic/well ties.

We developed a fracture model, which is able to handle both fracture anisotropy and shale anisotropy. We applied our fracture model to an East Texas well to demonstrate the anisotropic behavior of carbonate rocks with one set or two sets of

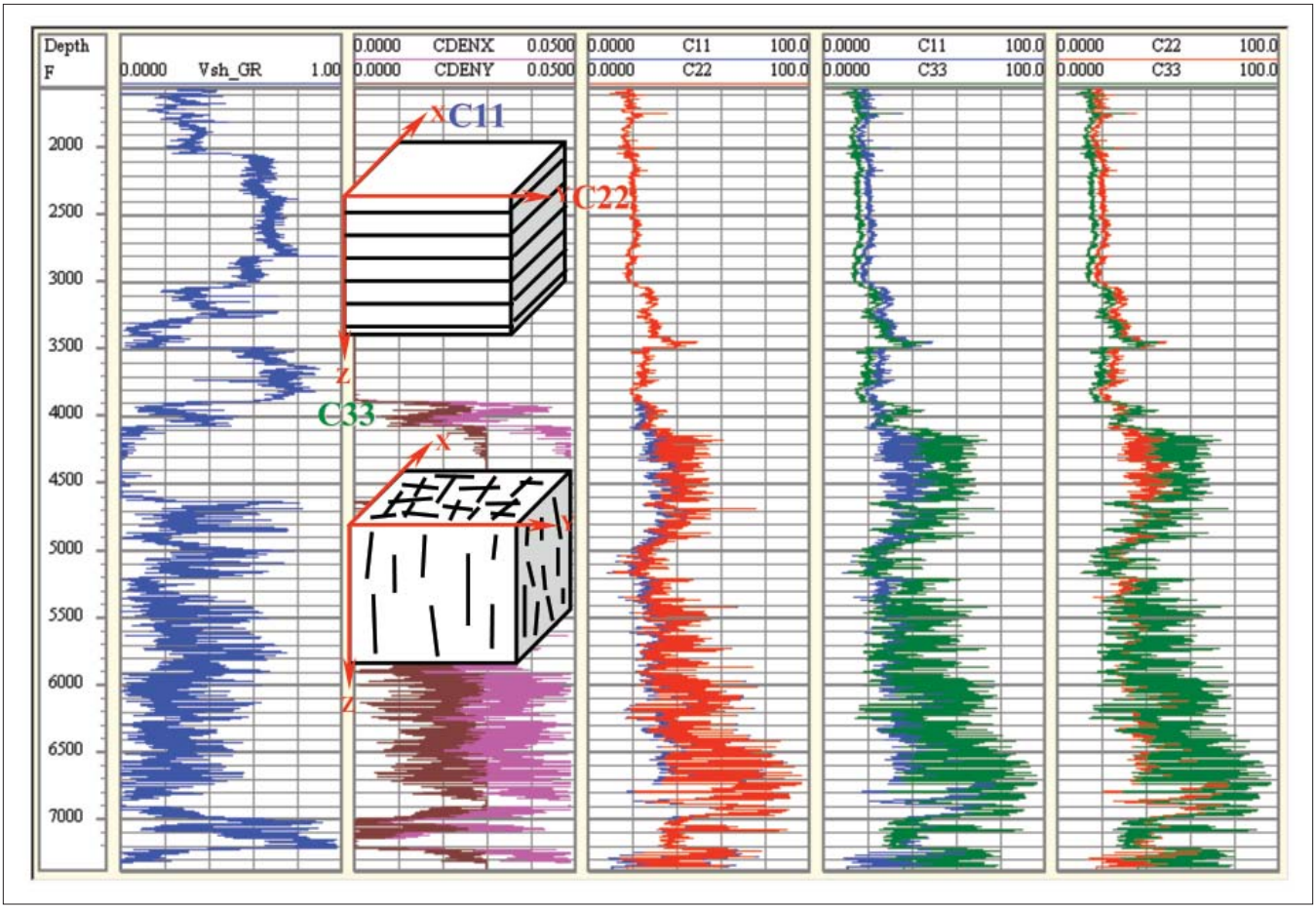

Figure 9. *Illustration of the effect of two vertical fracture sets on seismic anisotropy. Vsh_GR is shale volume estimated from the gamma-ray log, CDENX and CDENY are fracture densities in x and y directions; C11 (blue), C22 (red), and C33 (green) are elastic constants in x, y, and z directions, respectively.*

fractures. Our results show that azimuthal seismic anisotropy for fracture detection is most effective in the case of one single set of fractures.

Suggested reading. "Sonic velocity in carbonates—a combined product of depositional lithology and diagenetic alterations" by Anselmetti and Eberli (in *Subsurface Geology of a Prograding Carbonate Platform Margin, Great Bahama Bank: Results of the Bahamas Drilling Project*, SEPM Special Publication, 2001). "Controls on sonic velocity in carbonates" by Anselmetti and Eberli (*Pure and Applied Geophysics*, 1993). "The role of macroporosity and microporosity in constraining uncertainties and in relating velocity to permeability in carbonate rocks" by Baechle et al. (SEG 2004 *Expanded Abstracts*). "Changes of shear moduli in carbonate rocks: Implications for Gassmann applicability" by Baechle et al. (*TLE*, 2005). "Rock physics—The link between rock properties and AVO response" by Castagna et al. (in *Offset-Dependent Reflectivity—Theory and Practice of AVO Analysis*, SEG, 1993). "Factors controlling elastic properties in carbonate sediments and rocks" by Eberli et al. (*TLE*, 2003). "Pore shape effect on elastic properties of carbonate rocks" by Kumar and Han (SEG 2005 *Expanded Abstracts*). "Velocity and attenuation of seismic waves in two phase media: Part 1: Theoretical formulation" by Kuster and Toksöz (GEOPHYSICS, 1974). "Petroacoustic of carbonate reservoir rocks" by Rasolofosaon et al. (*TLE*, 2008). "The elastic properties of carbonates" by Sayers (*TLE*, 2008). "Seismic velocities in carbonate rock" by Wang et al. (*Canadian Journal of Petroleum Technology*, 1991). "Seismic properties of carbonate rocks" by Wang (in *Carbonate Seismology*, SEG, 1997). "A new velocity model for clay-sand mixtures" by Xu and White (*Geophysical Prospecting*, 1995). "A physical model for shear-wave velocity prediction" by Xu and White (*Geophysical Prospecting*, 1996). "Integrated Anisotropic Rock Physics Model" by Xu et al. (International Application Number: PCT/US2005/039002, 2006). TLE

Acknowledgments: We thank ExxonMobil US Production and the University of Miami for the use of their data in this article; Ganglin Chen for his work on fracture analysis and seismic modeling at the tight gas-sand well; and Yaping Zhu, Gregor Baechle, and Enru Liu for useful discussions.

Corresponding author: shiyu.xu@exxonmobil.com